Radome Shape Impact on Automotive Radar Sensor Operating at 79 GHz

Nebojša Pupavac and Miodrag Tasić, *Member, IEEE*

***Abstract*—At high frequencies radome (Radar Dome) degrades the automotive radar performance significantly. To gain better understanding of this phenomenon the radome shape and its impact on radiation pattern of the radar antenna array is analyzed in this paper. To analyze the impact of the radome shapes, an array of printed antennas is simulated with two different radome shapes and compared against the radiation pattern simulated without any radome. A simple single patch antenna for 79 GHz is designed using WIPL-D software platform, which was used for simulation of the antenna array with and without radome.**

***Index Terms*—Radome; radar sensor; antenna array; patch antenna.**

I. Introduction

A radome (radar dome) is a protective shield that encloses mmWave radar sensors and the antenna. It protects the antennas and electronics from external environment effects. The radome should be designed to minimally attenuate the electromagnetic signals transmitted and received by the antennas and as such should effectively be transparent to radio waves.

Since short range automotive radars work in 77-81 GHz frequency range [1], wavelengths of radar signals are rather small (3.75 mm at 80 GHz). This can cause significant interactions between radar signals and the plastic parts of the vehicle (painted bumper) and/or used radome, resulting in unpredictable error in the angle of arrival estimation [2]. Sometimes a calibration of the system can include the radar itself [3], but in the most cases radome is designed separately, with a goal to minimize reflections [4].

Although there are some general guidelines for automotive radar design [5], an electromagnetic simulation is necessary step in this process. In this paper we present results of the electromagnetic simulations for two radomes scenarios: spherical radome and rectangular radome, covering microstrip patch array. We will compare radiation patterns of these two systems with the radiation pattern of the microstrip patch array without the radome. The results can be used as a starting point in finding the optimal radome shape for a particular automotive radar design.

Nebojša Pupavac is with the School of Electrical Engineering, University of Belgrade, 73 Bulevar kralja Aleksandra, 11020 Belgrade, Serbia (e-mail: nebojsapupavac@gmail.com), (https://orcid.org/0000-0001-7851-7649)

Miodrag Tasić is with the School of Electrical Engineering, University of Belgrade, 73 Bulevar kralja Aleksandra, 11020 Belgrade, Serbia (e-mail: tasic@etf.bg.ac.rs), (https://orcid.org/0000-0002-8356-1190)

II. Guidelines for Radome Design

Since the most radomes are designed out of perfect dielectric material (with the relative permeability equal to 1, and the conductivity which is close to 0), main parameters for selecting appropriate material are relative permittivity and the loss tangent. The lower loss tangent provides the smaller attenuation by the radome, and overall smaller effect of the radome on the antenna performance. In finding optimal relative permittivity and a shape of the radome, the electromagnetic theory of time-harmonic electromagnetic fields for the plane-wave assumption can be used.

Electromagnetic wave reflections occur at the boundaries of the plane of mismatch. The plane of mismatch is the boundary of two domains with different dielectric permittivity. The interaction of the electromagnetic wave at the boundaries leads to the reflection and transmission of waves, quantized in terms of reflection coefficient *R*,

$$R = \frac{\sqrt{\varepsilon_{r1}} - \sqrt{\varepsilon_{r2}}}{\sqrt{\varepsilon_{r1}} + \sqrt{\varepsilon_{r2}}}, \tag{1}$$

and transmission coefficient *T*,

$$T = \frac{2\sqrt{\varepsilon_{r1}}}{\sqrt{\varepsilon_{r1}} + \sqrt{\varepsilon_{r2}}}. \tag{2}$$

Expressions (1) and (2) hold for an incident plane wave normal to the infinite flat boundary between the domains with relative permittivities ε_{r1} and ε_{r2} [6]. These expressions indicate that lower relative permittivity of radome dielectric material causes lower degradation of radar performance (since the other domain is air, with relative permittivity close to 1). However, optimal radome material needs to provide adequate mechanical characteristics, and the boundary in the general case is not a flat surface. Therefore, the selection of the dielectric material is always a tradeoff.

The radome thickness is particularly important for optimal performance of the automotive radar sensors. To avoid reflection at the radome wall, its thickness should be equal to an integer multiple, *n*, of the half of the wavelength in the radome [6]:

$$t_{opt} = n\frac{c_0}{2 f_r \sqrt{\varepsilon_r}}, \tag{3}$$

 ISBN 978-86-7466-930-3

where c_0 is speed of light in vacuum, ε_r is relative permittivity of radome material, and f_r is central frequency.

Typical parameters for the radome materials are shown in Table I. For radome shape analyses PTFE is selected as optimal solution which could be fabricated and tested to confirm simulation results presented in this paper. For $\varepsilon_{rPTFE} = 2$ and $f_r = 79\,\text{GHz}$, the optimal thickness of radome material from (3) is obtained for $n = 2$, $t_{opt} = 2.68\,\text{mm}$ (since the radome has to be at least 2 mm thick). Note that (3) is valid for electromagnetic plane waves at infinite flat boundary.

TABLE I
TYPICAL RADOME MATERIALS

Material	Relative Permittivity (ε_r)	Loss tangent tg(δ)
Polycarbonate	2.9	0.012
ABS	2.0-3.5	0.0050-0.019
PEEK	3.2	0.0048
PTFE	2	<0.0002
Plexiglass	2.6	0.009
PE	2.3	0.0003
PBT	2.9-4.0	0.002

The optimal distance between the antenna and the internal surface of the radome helps to minimize the effects of reflections caused by the radome. These effects become minimal if the waves returned to the antenna are in phase with the transmitted waves. So, the optimal distance between antenna and radome is [5]:

$$d_{opt} = m\frac{c_0}{2 f_r}. \tag{4}$$

For $m = 7$ we have $d_{opt} = 13.29\,\text{mm}$. A spherical radome in that case would have inner diameter of $26.58\,\text{mm}$, which is sufficient to cover the whole automotive radar sensor, including all necessary components.

III. ANTENNA DESIGN

We will model typical automotive radar sensors at 79 GHz, with four microstrip patch antennas. The layout of the single patch antenna is shown in Fig. 1. A substrate thickness is $t = 127\,\mu\text{m}$, with relative permittivity $\varepsilon_r = 3$, and loss tangent $\tan\delta = 0.0017$.

The patch width (W) and length (L) are calculated using the standard approximation [7],

$$W = \frac{c_0}{2 f_r \sqrt{\frac{\varepsilon_r + 1}{2}}}, \tag{5}$$

$$L = \frac{c_0}{2 f_r \sqrt{\varepsilon_{eff}}}, \tag{6}$$

where ε_{eff} is given by

$$\varepsilon_{eff} = \frac{\varepsilon_r + 1}{2} + \frac{\varepsilon_r - 1}{2}\left(1 + 12\frac{t}{W}\right)^{-\frac{1}{2}}. \tag{5}$$

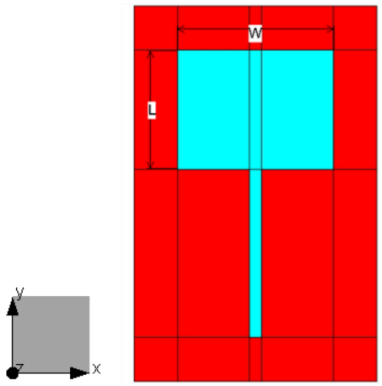

Fig. 1. Single rectangular patch antenna.

Antenna matching is achieved by adjusting the length of 0.1 mm wide feeding line using software package for electromagnetic modeling WIPL-D Pro [8]. Parameter s_{11} over desired frequency bandwidth is shown in Fig. 2, whereas radiation pattern in H-plane and E-plane is shown in Fig. 3.

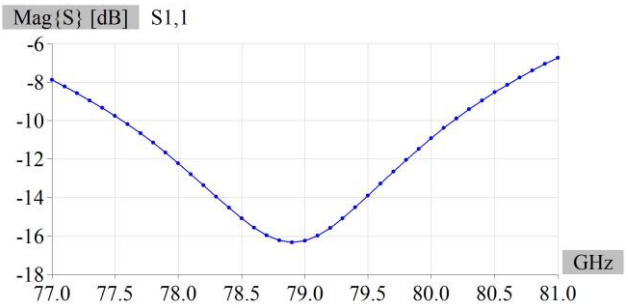

Fig. 2. Parameter s_{11} for a single microstrip patch antenna.

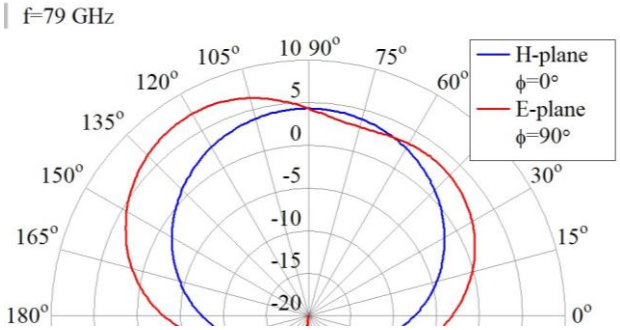

Fig. 3. Radiation pattern (Gain in dB) for a single microstrip patch antenna.

 ISBN 978-86-7466-930-3

Typical automotive radar sensors at 79 GHz are using 3 Tx and 4 Rx antennas. In this simulation only Rx antenna is simulated. It is made of four single microstrip patch antennas shown in Fig. 1, with λ/2 spacing, as shown in Fig. 4.

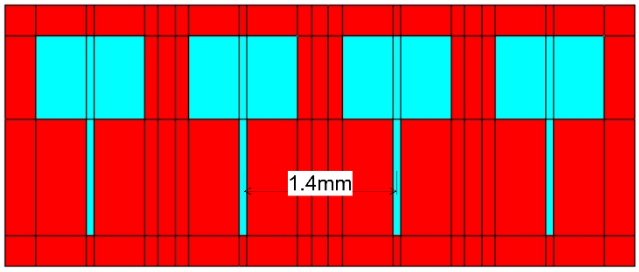

Fig. 4. Antenna Array with λ/2 spacing.

Since the array is symmetrical, only first two antennas (from left to right) are connected to generators, G1 and G2. The third and fourth antennas are symmetrical, so it is assumed that inner antennas have identical, but mirrored radiation pattern, as well as the outer antennas.

Fig. 5 shows that H-plane radiation patterns of both inner and outer antenna are deformed compared to the radiation pattern of a single antenna from Fig. 3 (where H-plane radiation pattern was symmetrical). Inner antenna deformation is less significant because it is surrounded by identical antennas from both left and right side.

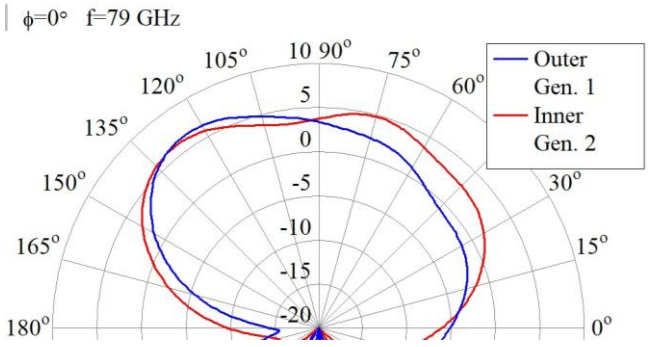

Fig. 5. Inner and Outer Antenna Radiation Patterns in H-plane.

IV. Antenna Array With Radome

Antenna array with a spherical radome of radius $d_{\text{opt}} + t = 13.42$ mm, with the center in the center of the array, is shown in Fig. 6.

Antenna array with a rectangular radome, with the same distance from the antenna array, having square cross section with the same width as the sphere radome diameter is shown in Fig. 7.

Both radomes are made from the material with relative permittivity 2 and thickness $t_{\text{opt}} = 2.68$ mm.

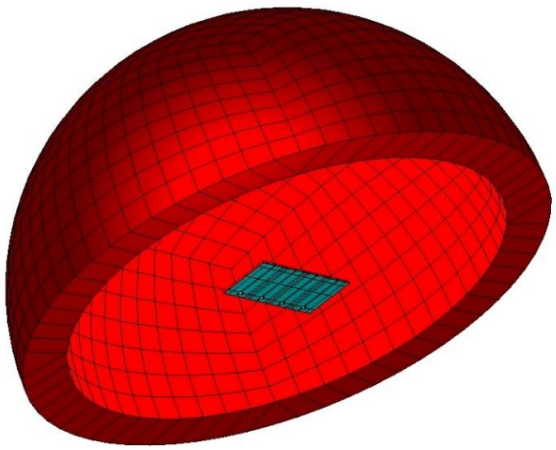

Fig. 6. Antenna array with the spherical radome.

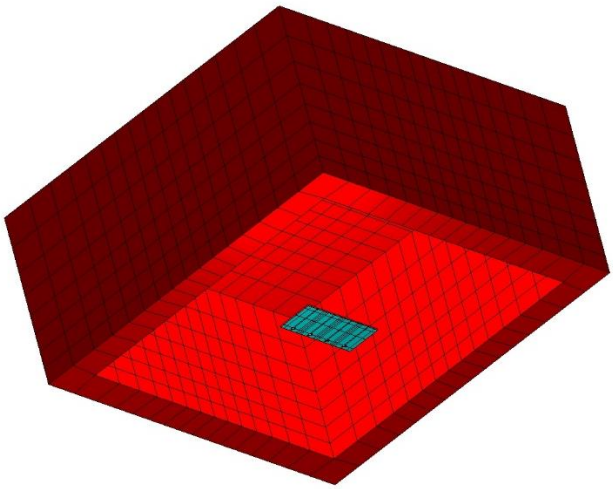

Fig. 7. Antenna array with the rectangular radome.

The electrical distance through the radome in boresight is equivalent to the thickness of the radome wall. The radome wall thickness t_{opt} is designed to cancel reflections from the radome, but in the case of normal incidence of the electromagnetic plane wave on infinite flat boundary Therefore, at boresight of the radome, the reflections at the inner wall will mainly cancel, resulting in low net reflections.

In the case of a rectangular (flat) radome, when moving away from the boresight to higher grazing angles of arrival, the distance traveled by the mmWave signal is greater than "optimal thickness", as illustrated in Fig. 8. This causes multiple reflections at the radome interface boundary resulting in ripples in the antenna radiation patterns and leading to nulls. These ripples and nulls can cause inconsistency in the detection of the objects at higher grazing angles resulting in angle estimation errors.

In the case of the spherical radome, the radome performance at different grazing angles will be more similar to the performance at boresight.

 ISBN 978-86-7466-930-3

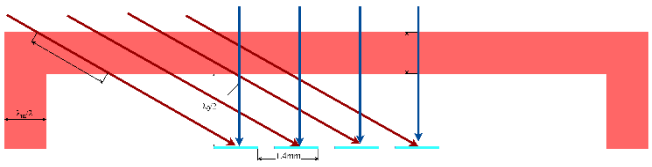

Fig. 8. Cross sectional view of the rectangular radome and the antenna array.

Radiation patterns of the outer antenna in E-plane, without a radome, and with spherical and rectangular radomes are shown in Fig. 9, whereas the similar graph for the inner antenna is shown in Fig. 10.

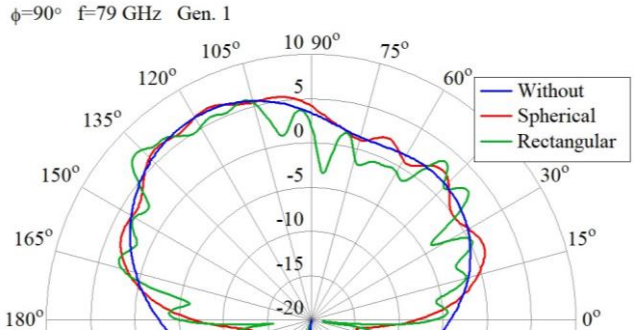

Fig. 9. Outer antenna radiation pattern in E-plane.

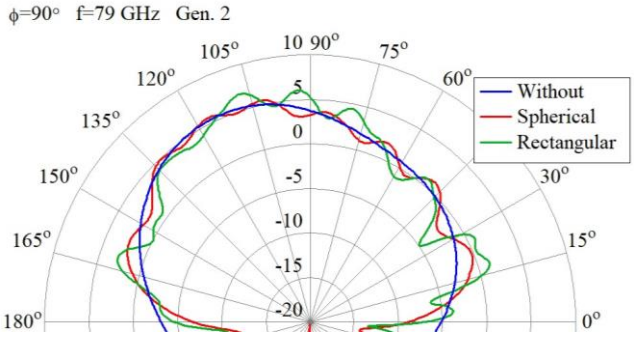

Fig. 10. Inner antenna radiation pattern in E-plane.

Radiation patterns of the outer antenna in H-plane, without a radome, and with spherical and rectangular radomes are shown in Fig. 11, whereas the similar graph for the inner antenna is shown in Fig. 12.

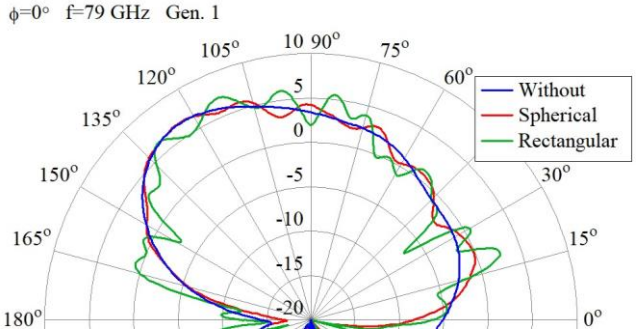

Fig. 11. Outer antenna radiation pattern in H-plane.

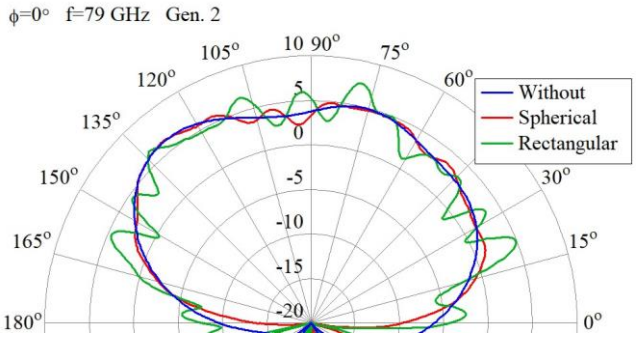

Fig. 12. Inner antenna radiation pattern in H-plane.

The radiation pattern from 180° to 360° is not interesting for the radar performance, also the simulation result is not relevant as the model doesn't include the complete PCB which is in realty much larger and has many components which are not modeled and neglected for the antenna simulation.

For the most applications azimuth angle of arrival estimation is more important. Therefore, the radiation patterns for H-plane (azimuth plane) are also shown in Cartesian system, in Figs. 13 and 14, to emphasize the ripples caused by radomes and to show the difference between the two radome shapes. Expected field of view of the automotive sensor is around ±60°, so antenna patterns from 15° to 165° are shown.

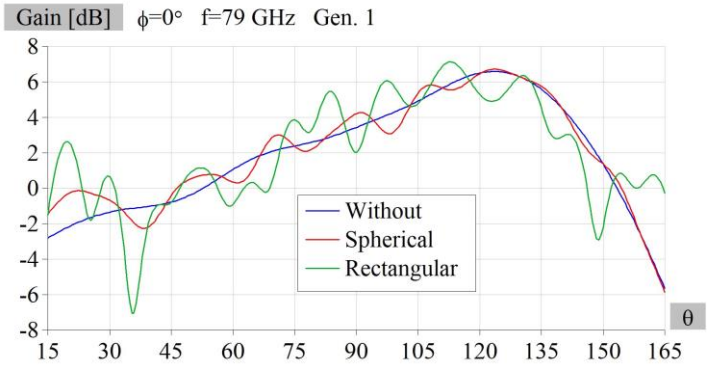

Fig. 13. Outer antenna radiation pattern in H-plane (Cartesian).

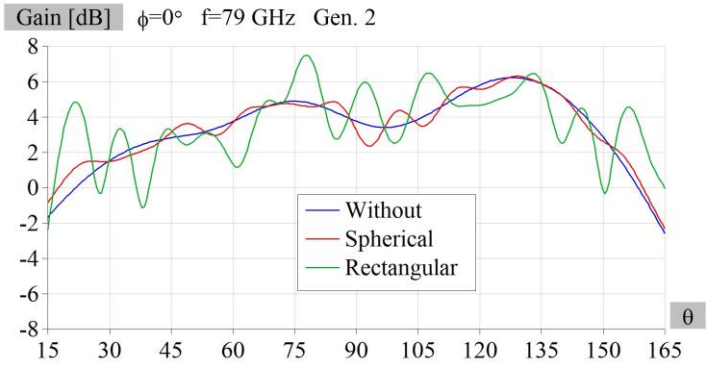

Fig. 14. Inner antenna radiation pattern in H-plane (Cartesian).

 ISBN 978-86-7466-930-3

V. CONCLUSION

The aim of these simulations was to show weather the radome shape could improve automotive radar sensor performance and if it makes sense to invest in designing more complicated radome shapes compared to the most common rectangular design. The simplified model comprising of only 4 Rx antennas (typically mmWave sensors are using 4 Rx and 3 Tx antennas) is showing that spherical radome has significantly reduced ripples compared to the flat radome.

Also, the spherical radome cannot fulfill half wavelength conditions for each antenna, so some of the ripples still appear comparing to the scenario without a radome.

Main influence of the above-mentioned ripples is the degradation of the radar performance by means of angle of arrival estimation and the maximal detection range. To confirm the simulation results, a realistic antenna array with both Rx and Tx antennas should be measured using Vector Network analyzer (VNA) and referent (horn) antenna using different radomes. Also, the complete mmWave sensor with the identical antenna array and targets at different angle of arrival could be tested to indicate the angle estimation accuracy degradation introduced by different radomes and compared with the radar simulation results.

REFERENCES

[1] K. M. Strohm, H. L. Bloecher, R. Schneider and J. Wenger, "Development of future short range radar technology," *European Radar Conference, 2005. EURAD 2005.*, 2005, pp. 165-168.

[2] M. M. S. Hossain *et al*., "Wideband Radomes for Millimeter-Wave Automotive Radars," in *IEEE Transactions on Antennas and Propagation*, vol. 70, no. 2, pp. 1178-1186, Feb. 2022.

[3] S. Buitrago, S. Blanch and J. Romeu, "Automotive radar and radome calibration to improve the direction of arrival detection performance," *12th European Conference on Antennas and Propagation (EuCAP 2018)*, 2018, pp. 1-5.

[4] F. Fitzek and R. H. Rasshofer, "Automotive Radome Design - Reflection Reduction of Stratified Media," in *IEEE Antennas and Wireless Propagation Letters*, vol. 8, pp. 1076-1079, 2009.

[5] C. K., H. U. R. M. and G. P. Authors, “mmWave Radar Radome Design Guide,” TI, Dallas, Texas, USA, 2021.

[6] A. Đorđević, *Elektromagnetika*, Akademska misao, Beograd,2008.

[7] A. Pandey, *Practical Microstrip and Printed Antenna Design*, Artech House. 2019.

[8] https://wipl-d.com/products/wipl-d-pro/.

 ISBN 978-86-7466-930-3